ON THE IDENTIFICATION OF SOLID SOUND SOURCES VIA THE FFOWCS WILLIAMS-HAWKINGS INTEGRAL

P. R. Spalart
Boeing Commercial Airplanes, Seattle, USA, philippe.r.spalart@boeing.com

The Ffowcs Williams-Hawkings (FWH, [1]) formula shown here in its far-field approximation (eqn. 1) is extremely valuable in computational aeroacoustics, and is widely used to post-process unsteady simulations, in order to calculate the sound at distances beyond the accurate range of the numerical grid. The formula distinguishes the monopole and dipole contributions from the solid surfaces Σ (third and second lines) and that from the quadrupoles present in the fluid (first line). Curle showed that at low Mach numbers, the solid-surface terms dominate [2]. Furthermore, for compact sources, the unsteady force on the body dominates. Very few studies have explicitly included the quadrupoles in the volume, but many have used a permeable FWH surface Σ, which in principle surrounds the quadrupoles, giving valid results independent of Mach number. However, in spite of some serious doubts over the solid-surface approach [3], many people in the field prefer using it, partly due to simplicity and partly because of some difficulties associated with turbulence crossing the permeable surface.

$$\begin{aligned} 4\pi|\mathbf{x}|(1-M_r)\,p'(\mathbf{x},t) = {} & \frac{x_j x_l}{|\mathbf{x}|^2 c_0{}^2}\frac{\partial^2}{\partial t^2}\int_V \{T_{jl}\}_{ret}\, dV \\ & + \frac{x_j}{|\mathbf{x}| c_0}\frac{\partial}{\partial t}\int_\Sigma \{p' n_j + \rho u_j (u_n - U_n)\}_{ret}\, d\Sigma \\ & + \frac{\partial}{\partial t}\int_\Sigma \{\rho_0 u_n + \rho'(u_n - U_n)\}_{ret}\, d\Sigma \end{aligned} \tag{1}$$

Our purpose is to explore these effects, using two model problems. An additional attraction of the solid-surface approach is the idea of identifying the “true” source of the sound by computing separately the integrals for different components; in a landing gear, one may ask whether the wheel, the door, the post or the cavity “makes more noise,” and is therefore the better candidate for noise-reduction technology [4, 5]. We wish to determine whether this “self-evident” argument gives a rigorous and effective approach. Our focus is on airframe noise, because the neglect of quadrupoles is much less defendable for engine noise. One key feature is the shielding of sound towards various directions; any approach that fails to reflect this shielding will be suspect.

Our first problem does not involve quadrupoles, but leads to the identification of sound sources, and shielding. As shown in Fig. 1a, a dipole is placed under a sphere. This is a generic model for an aircraft component such as a wheel applying an unsteady force to the fluid. The “straightforward” identification approach would calculate the solid-FWH sound field, and declare that “this is the sound of this part of the airplane.” Here, the sound field of the dipole is known analytically. The dipole is injected into the flow field over a small volume, and is therefore “a compact source.” We only show cases with a vertical dipole (F_y), but results with a horizontal dipole led to the same conclusions.

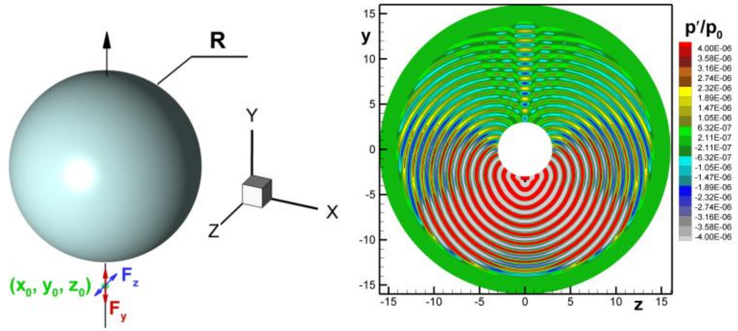

Fig. 1 Dipole placed under sphere. Left, geometry; right, pressure field

There is no flow, and the walls are treated as free-slip surfaces. The parameters are as follows: the wave-length is 1/3 times the sphere radius R, and the dipole is ½ a wave-length away from the surface. This creates interference patterns with 45 degrees for the dominant direction, as seen in Fig. 1b; other cases, with different offsets for the dipole, produced different patterns. As could be expected, the shielding by the sphere in the upward direction is very definite.

We now turn to quantitative results, comparing the sound at a distance of 11 wave-lengths λ from the origin. A FWH utility, valid in the near-field, was provided by Drs. A. Dyben and T. Kozubskaya of Keldysh Institute of Applied Mathematics (Moscow) and allows comparisons with the direct output of the simulation, where the grid is still fine; the same conclusions would be reached for far-field sound, but the simulation cannot provide that, since the grid coarsens for large r (and a sponge layer was introduced). In Fig. 2a the simulation result, in magenta, confirms the interference pattern and the shielding seen in Fig. 1b. The peak level at ±45 degrees is 25dB higher than the lowest level, in the straight-up direction. This result is accurately reproduced by the permeable

FWH formula, independently of the radius of the FWH sphere (blue and green curves). The sound field of the dipole itself (black), in contrast, does not reproduce shielding; the only difference between the up and down direction is due to the difference in distance (14.5 λ versus 7.5 λ). It also misses the interference patterns. The sound field of the dipole with an opposite image dipole inside the sphere (not shown) does capture interference, to leading order, but that does not provide a very practical method.

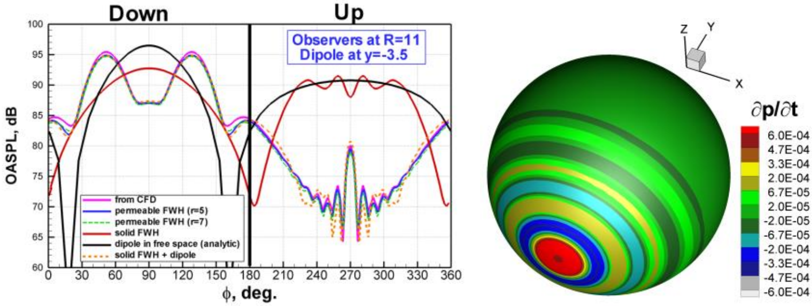

Fig. 2. Left, sound extracted from simulation, and produced by integral formulas. Right, FWH surface term on the sphere

Of more interest are the results of the sphere's solid-surface contribution, in red, and its combination with the dipole, in orange. In the upwards direction, the two almost cancel. This combination gives a very accurate answer, almost as good as the permeable formula. On a theoretical basis, this may be unsurprising, since this problem has no quadrupoles. However, in practice, this shows that while the dipole is the true source of sound, the calculation of the sound field must include the sphere's contribution, which in practice would mean the airplane's fuselage and wing. Figure 2b shows the FWH integrand on the sphere, in other words the "footprint" of the dipole. Its extent appears to be a few times the distance from the dipole to the surface.

Next, a generic fuselage with a simplified landing-gear cavity is considered, as illustrated in Fig. 3. This flow having quadrupoles, the results may not be as close to perfection as in the first case, but we expect strong effects of shielding, with the approach separating various parts of the surface in the FWH integral possibly leading to paradoxes.

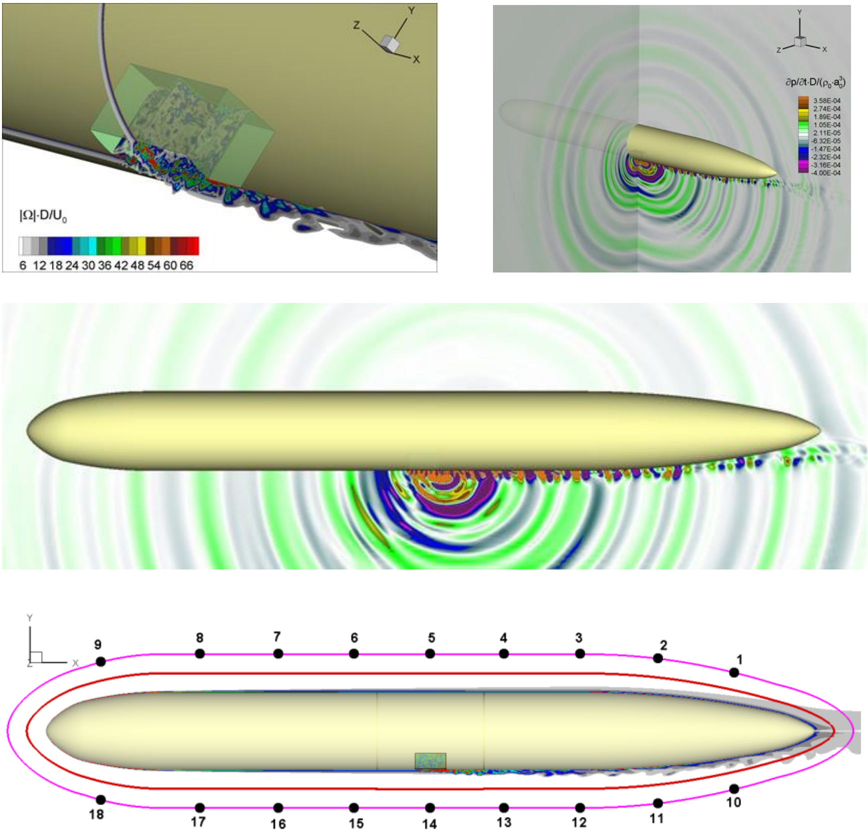

Fig. 3. Simplified landing-gear cavity. Top left, vorticity contours; top right and middle, pressure field (time derivative); bottom, permeable surfaces

The flow is treated with Delayed Detached-Eddy Simulation, with most of the fuselage boundary layer in quasi-steady RANS mode, and strong clustering of the grid near the cavity. The Mach number is 0.25 and the Reynolds number based on fuselage diameter D is 10^7. The simulation produces the expected highly unsteady shear layer bounding the cavity, and weaker but fine-scale vorticity in it. Turbulence then propagates along the body. The pressure field is marked by waves with a wavelength slightly longer than D (somewhat controlled by grid spacing).

Figure 4 shows that the permeable-surface FWH formula reproduces the sound in the simulation very accurately. This includes the strong sheltering, since the sound level at Point 5, above the body, is about 25dB lower than at

Point 14, below it. On the other hand, the spectrum shape for low frequencies is very similar at those two points, which we have not explained yet.

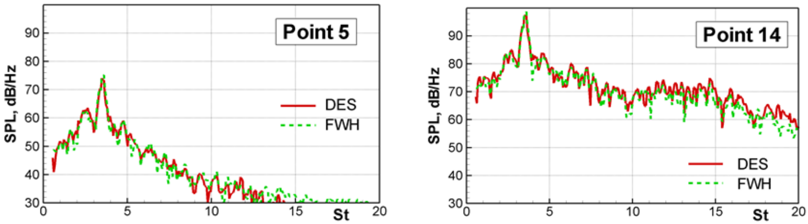

Fig. 4. Spectra from simulation and from permeable-surface integral at two points above and below fuselage (see Fig. 3)

Figure 5 presents results in the upwards and downwards direction, which are not as simple as for the sphere-dipole case. The difference between directions is weaker than in Fig. 4, around 8dB, due to this applying in the far field.

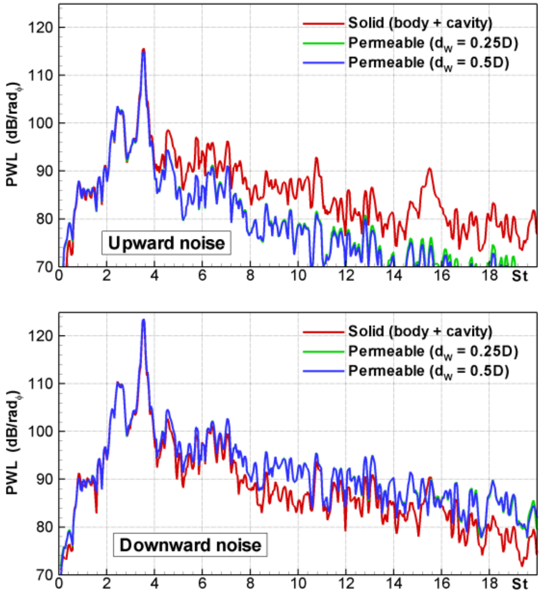

Fig. 5. Sound power levels in the vertical direction with different FWH approaches. Far-field results. Upper graph: upwards; lower graph: downwards

The solid and permeable results in Fig. 5 are almost identical up to a Strouhal number of 4, and in particular the peak at *St* ~ 3.5 is identical. Given a

Mach number of 0.25, this corresponds although loosely with the dominant wave of Fig. 3. For *St* larger than 4, the two results diverge, and the solid-FWH calculations essentially miss the shielding effect, even though these are results with the full surface (cavity and fuselage skin), an approach which was successful for the sphere-dipole case. This appears to reflect the quadrupole contribution, which would have constructive interference with the surface terms in one direction, and destructive interference in the other direction. The relative success of the solid formula for low frequencies (which would not be relevant in airline practice) has not been explained yet; in particular, a simple argument such as the source being compact does not seem to apply since $\lambda \sim D$.

The dominant frequency is of interest. If we assume that the large eddies in the mixing layer propagate at half the freestream velocity, $St = 3.5$ corresponds to an eddy spacing of $D/7$, which is larger than the visual spacing in the simulation. The Strouhal number based on cavity length L is 1.4, which would approximately correspond with the third Rossiter mode (using $St_L=(n-\gamma)/(\mathrm{M}+1/\kappa)$ with $\gamma=0.25$ and $\kappa=0.57$). This is not very conclusive. Finally, the cavity length and depth are 0.4 D and 0.2 D, respectively, so that conjectures based on half- or quarter-wavelength modes are not satisfied either.

Overall, our results strongly support the permeable-surface FWH formula, and indicate that the solid-surface formula can be misleading regarding the actual sources of sound, and in particular fail to capture directional effects.

Acknowledgements

Calculations and scientific discussions provided by Drs. M. Shur, M. Strelets and A. Travin of St. Petersburg Polytechnic University and NTS, Russia. The calculations were performed at the Computer Center “Polytechnichesky”.

References

1. J.E. Ffowcs Williams, D.L. Hawkings. Sound generation by turbulence and surfaces in arbitrary motion. *Phil. Trans. Roy. Soc. A*, 1969, 264-321.
2. N. Curle. The influence of solid boundaries upon aerodynamic sound. *Proc. Roy. Soc.* **A231**, 1955, 505-514.
3. P.R. Spalart. On the precise implications of acoustic analogies for aerodynamic noise at low Mach numbers. *J. Sound Vib*. **332**, 2013, 2808-2815.
4. J.-C. Giret. Simulations aux grandes échelles des écoulements instationnaires turbulents autour des trains d’atterrissage pour la prédiction du bruit aérodynamique. Thesis, INP Toulouse, May 2014
5. P.R.G. de Azevedo Jr, W.R. Wolf. Noise Prediction of the LAGOON Landing Gear Using Acoustic Analogy and Proper Orthogonal Decomposition. AIAA-2016-2768.